MASTER FINAL PROJECT

Development of chitosan/heparin nanoparticles for targeted antimalarial drug delivery

Lucía Gutiérrez Chamorro

Supervisor: Xavier Fernández Busquets

Institute for Bioengineering of Catalonia (IBEC)

Barcelona Institute for Global Health (ISGlobal)

Abstract

Malaria, a life-threatening disease caused by parasites of the genus *Plasmodium*, is one of the most prevalent parasitic diseases in the world. Keeping in mind that an effective vaccine against malaria is still under development, chemotherapy is one of the most important strategies to reduce its associated morbidity and mortality. However, the emergence of drug-resistant malaria parasites, combined with the non-specific targeting of current chemotherapies to intracellular parasites, highlights the necessity of new therapeutic and drug delivery approaches, like novel antimalarial drugs and improved methods for their efficient administration. In this context, nanomedicine enables numerous potential opportunities for malaria treatment such as nanovector-based drug delivery strategies. Polysaccharides, in particular chitosan -a deacetylated chitin derivative-, have gained increasing attention because of their numerous advantages. In addition, data from single-molecule force spectroscopy and fluorescence microscopy have shown binding specificity of heparin to *Plasmodium*-infected red blood cells *vs.* non-parasitized erythrocytes.

The aim of this project is to establish a method for the synthesis of antimalarial drug-loaded chitosan/heparin nanoparticles and evaluate their specific antimalarial activity. For this purpose, nanoparticles are prepared by the ionic gelation method. In order to characterize them, we use scanning electron microscopy and dynamic light scattering. Finally, growth inhibition assays in *Plasmodium falciparum* cultures are performed to determine antimalarial activity and targeting of the nanoparticles to parasitized red blood cells.

In conclusion, we explore a new cost-efficient approach for the treatment of malaria based on a nanomedical strategy that could provide a targeted delivery contributing to reducing resistance evolution.

<p style="text-align:center">**INDEX**</p>

List of abbreviations

ACT: artemisinin-combination therapy

Ch: chitosan

CQ: chloroquine

DLS: dynamic light scattering

FBS: fetal bovine serum

GAGs: glycosaminoglycans

GIAs: growth inhibition assay

HCl: hydrochloric acid

Hep: heparin

HUVEC: human umbilical vein endothelial cells

IBEC: Institute for Bioengineering of Catalonia

IC_{50}:   median inhibition concentration

KCl: potassium chloride

MHD: mean hydrodynamic diameter

NaCl: sodium chloride

nm: nanometres

NPs: nanoparticles

P. falciparum: *Plasmodium falciparum*

PBS: phosphate-buffered saline

PDI: polydispersity index

pRBC: parasitized red blood cells

RBC: Red blood cells

Rcf: relative centrifugal force

SEM: scanning electron microscopy

WHO: World Health Organization

1. Introduction

Malaria is a life-threatening disease caused by parasites of the genus *Plasmodium*. There are approximately 156 named species of *Plasmodium* which infect various species of vertebrates, but only five infect humans: *P. falciparum*, *P. vivax*, *P. ovale*, *P. malariae* and *P. knowlesi*. (1) (2). *P. falciparum* is the most prevalent malaria parasite on the African continent and it is responsible for most malaria-related deaths globally (3). Malaria is difficult to recognize as the first symptoms -fever, headache, chills and vomiting- may be mild. It is preventable and curable, but if left untreated, it can develop to severe complications often leading to death (2). Although increased prevention and control measures have led to a reduction in mortality rates by 60%, according to the latest World Health Organization (WHO) estimates, there were 212 million new cases of malaria worldwide in 2015 and 429,000 malaria deaths, mostly children (3) (4).

All five *Plasmodium* species exhibit a similar and complex life cycle with only minor variations involving an insect vector (mosquito) and a vertebrate host (human) (Fig. 1). When a *P. falciparum*-infected female *Anopheles* mosquito bites, it injects sporozoites into the human blood stream. The parasites grow and multiply in the liver cells and mature into schizonts, which rupture and release merozoites. After this initial replication in the liver, parasites invade red blood cells (RBCs), where they develop first into rings, and then into the late forms trophozoites and schizonts. Schizont-infected RBCs burst and release more daughter parasites (merozoites) that continue the cycle by invading new erythrocytes. Some parasites eventually differentiate into sexual stages -female and male gametocytes- that could be picked up by an *Anopheles* mosquito during a blood meal and start another cycle of growth and multiplication. Soon after blood feeding, ingested parasite gametocytes produce male and female gametes that fertilise and form the zygotes. The zygotes become motile and elongated ookinetes which invade the midgut wall of the

mosquito where they develop into oocysts. The oocysts grow, rupture and release sporozoites, which migrate to the mosquito's salivary glands. The malaria cycle is restarted when sporozoites are injected into a human with the mosquito's next bite (5).
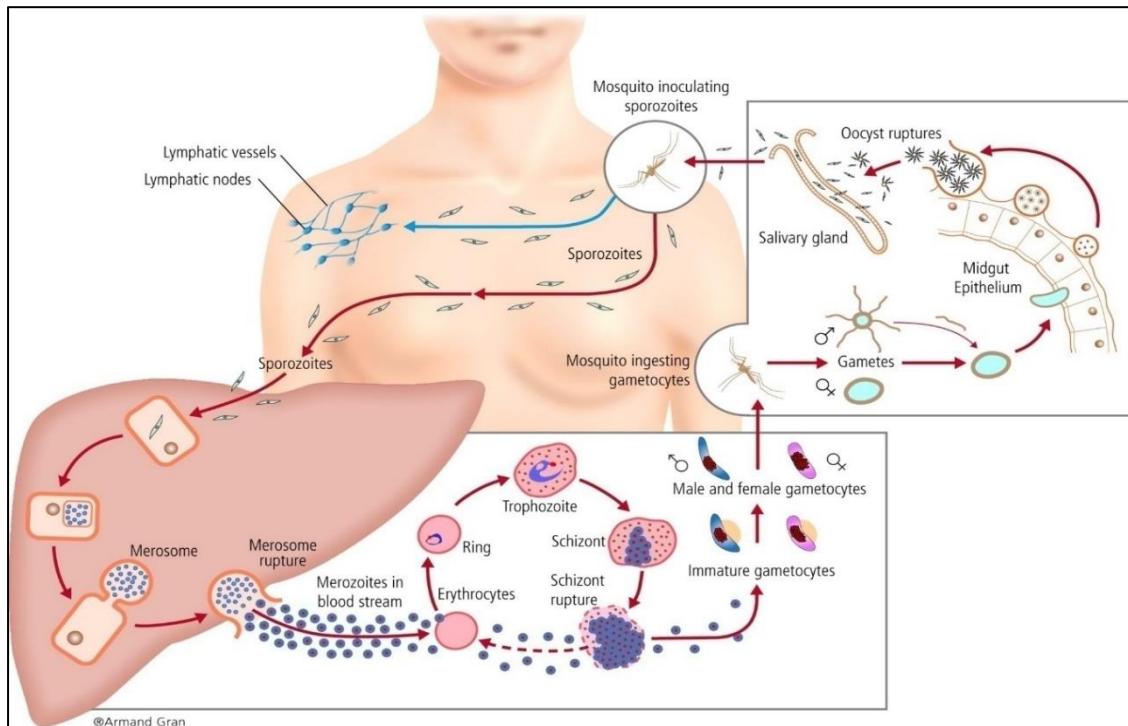

Figure 1. Malaria life cycle

Bearing in mind that an effective vaccine against malaria is still under development (5), today malaria treatment and control relies principally on the action of drugs against the asexual blood stages of the parasite. Currently, the best available treatment, particularly for *P. falciparum* malaria, is artemisinin-based combination therapy (ACT) (1). However, one of the main challenges in the present fight against malaria is the emergence of antimalarial drug resistances (6). This problem is complicated by cross resistance, in which resistance to one drug confers resistance to other drugs that belong to the same chemical family or which have similar modes of action. Parasite resistance results in a delayed or incomplete clearance of parasites from the patient's blood when the person is being treated with an antimalarial (5). Additionally, another important drawback associated with current available chemotherapy is the non-specific targeting to

intracellular parasites. The current delivery method of antimalarials ends up with the free compound in the bloodstream, where it can be absorbed by all cells, and not only by *Plasmodium*-infected red blood cells (pRBCs). Therefore, drugs could be removed by many tissues and organs before entering the target cells. This reduced specificity results in high drug dose requirements that can trigger undesirable side effects (7). On the other hand, reducing drug concentration to minimize undesirable side effects contributes to the evolution of resistance. For all those reasons, there is a pressing need for new therapeutic strategies against malaria, like novel antimalarial drugs and improved methods for their efficient administration or new targets for vaccines (7).

In this setting, nanomedicine, the application of nanotechnology to human healthcare, enables numerous potential pathways and a wide range of research opportunities to improve medical diagnosis and therapy in many fields, including malaria treatment (8). Although nanomedicine is a young science, it is at present a key medical technology, with increasing funding on a global basis and evolving and growing exponentially (9) (10). The origin of nanotechnology traces back to 1959 when the Nobel prize winner, Richard P. Feynman, introduced the idea in his paper *There's Plenty of Room at the Bottom. An invitation to enter a new field of physics.* Later on, in the late 1960s, Speiser developed the first nanoparticles for drug delivery purposes and for vaccines (11). Particularly for the treatment of malaria, it was in 1979 when Pirson *et al.* reported the first nanocarriers -liposomes- for antimalarial drug delivery (12) (13). In 1986, the first site-specific drug delivery method was developed by Gupta *et al.* with the design of liposomes capable of specifically targeting rat erythrocytes *in vivo* (14). At present, there are different types of nanocarriers, e.g. liposomes, dendrimers, micelles and polymers and a wide range of materials have been employed to prepare them. Nevertheless, they often have limitations due to non-selectivity issues. Antibody-functionalized nanovectors for targeted drug

4

delivery have been successfully reported. However, some of their properties, such as a lengthy and expensive production or a loss of targeting efficacy, limit their use as targeting elements in antimalarial therapeutic strategies (7) (15).

Polysaccharides have recently drawn increasing attention for nanomedical applications, in particular cationic polymers such as chitosan (a chitin derivative biopolymer consisting of α (1-4) 2-amino 2-deoxy β-D-glucan). Due to the availability of free amino groups, chitosan carries a positive charge and reacts with other anionic polymers (16). An increasing number of studies show that chitosan-based nanocarriers may be a promising and valid method for safe and efficient drug administration. Among the advantages of chitosan, its low toxicity and good biodegradability are the most important (17) (18). Heparin, a sulphated glycoconjugate, has been reported to have antimalarial activity. This is because heparin masks the apical surface of merozoites and blocks interaction with the erythrocyte membrane after initial attachment (19). However, it was abandoned as a treatment for malaria because of side effects due to its well-known anticoagulant activity (15). In addition, data from single-molecule force spectroscopy have shown binding specificity of heparin to pRBCs vs. RBCs (20). Thus, heparin electrostatically bound to preformed chitosan nanoparticles has reduced haemorrhagic activity and could act as antibody surrogate, having a dual activity as a pRBC-targeting molecule but also as an antimalarial drug in itself (21). Moreover, heparin electrostatically embedded in the nanoparticles is less prone to be released in the circulation, with the subsequent reduction of the risk of anticoagulation and internal bleeding (21).

Chloroquine (CQ), a 4-aminoquinoline drug, is well-known as an antimalarial agent. It was effective on all five species of human malaria parasites and therefore remained for a long time the main antimalarial treatment. CQ acts against intraerythrocytic stages of the human parasite, and is thought to exert its toxic effect in the parasite's acidic digestive

vacuole (16). Although widespread resistance to CQ exists and it is no longer administered in many malaria endemic countries, in this work, CQ is used for a proof-of-concept assay with the CQ-sensitive 3D7 *P. falciparum* strain.

2. Hypothesis and objectives

This study seeks to synthetize and characterise chitosan-heparin nanoparticles containing chloroquine. It is hypothesized that the nanoparticle carrier may protect the drug from degradation and increase its stability. In addition, because of the presence of heparin, which could have a dual role as antimalarial and as a targeting element, nanoparticles might specifically interact with *Plasmodium*-infected erythrocytes. With time, the nanoparticle might release the drug, which in this way could act locally on the infected erythrocytes.

In this study, nanoparticles composed of chitosan and heparin in various weight ratios are prepared and their characteristics examined with dynamic light scattering (DLS) and scanning electron microscopy (SEM). A possible cytotoxic effect of the nanoparticles is explored *in vitro* on human umbilical vein endothelial cells (HUVEC) with a cell viability assay (MTT assay). Finally, the antimalarial activity of the nanoparticles is determined by growth inhibition assays (GIAs).

3. Materials and methods

3.1 Chemicals and reagents

Chitosan (low molecular weight), heparin sodium salt from porcine intestinal mucosa, Kolliphor P188, chloroquine diphosphate salt, acetic acid, fetal bovine serum (FBS), HEPES, Giemsa stain, phosphate buffered saline (PBS) tablets and penicillin-streptomycin solution Stabil were purchased from Sigma. Sodium sulphate was obtained

from Merck. Ethanol and methanol were purchased from VWR. Medium 199 with Earle Salt with Glutamine was purchased from LabClinics.

3.2 Preparation of chitosan-heparin nanoparticles

Chitosan-heparin nanoparticles were prepared by a simple ionotropic gelation method under magnetic stirring at room temperature. In brief, the synthetic procedure involves the dissolution of 25 g chitosan in 100 mL of 2% v/v acetic acid solution containing 1% w/v Kolliphor P188. Under magnetic stirring at room temperature, 2 mL of heparin (0.25 mg/mL) was added into aqueous chitosan. About 2.5 mL of a 20% w/v sodium sulphate solution was added dropwise to the chitosan-heparin solution under magnetic stirring (1600 rpm), which was maintained for 1 h for the formation of nanoparticles. The products were collected through 3 cycles of centrifugation at 13,000 rcf for 45 min and re-dispersed in water. The supernatant was discarded and the nanoparticles were finally re-suspended in deionized water for further analysis.

3.3 Particle characterization

3.3.1 DLS study

The synthesized chitosan and chitosan-heparin particles were characterized by DLS. Particle size was measured and analysed with a dynamic light scattering analyser (Zetasizer Nano ZS90, Malvern Systems, IBEC, Barcelona). The analysis was performed at a scattering angle of 90˚ at 25˚C.

3.3.2 SEM analysis

The morphology of the synthetized nanoparticles (both chitosan and CQ-loaded chitosan-heparin nanoparticles) was observed using scanning electron microscopy (Nova NanoSEM 230, IBEC, Barcelona). Chitosan-heparin nanoparticles solutions were

sonicated for 15 min for a better particle dispersion and to prevent nanoparticle agglomeration. One drop of the nanoparticle solution was spread onto a silica slide which was then dried at room temperature for SEM analysis.

3.4 In vitro cytotoxicity determination of nanoparticles by MTT assay

The toxicity of the nanoparticles was assessed in HUVEC cells. The cells were maintained in medium 199 with Earle Salt with Glutamine and supplemented with 1% penicillin/streptomycin, 10% FBS, at 37°C in a 95% air, 5% CO_2 atmosphere in a CO_2 incubator. HUVEC cells were seeded into two 96-well plates (one for the 24 h and another one for the 48 h assay, see below) at a density of 50,000 cells per well, in 100 µL of complete media. After 24 h of incubation, nanoparticle samples were added to the cells at different concentrations (1, 0.1 and 0.01 mg/mL), and were incubated for 24 h and 48 h at 37°C. When incubation time was completed, 10 µL of WST-1 reagent was added. After 4 h at 37°C, cell viability was estimated by measuring A_{440} absorbance with a spectrophotometer (Epoch R Microplate Spectrophotometer, Bio Tek).

3.5 Drug loading of nanoparticles

A drug solution was prepared by dissolving 200 mg of CQ in 100 mL of deionized water, to which three or four drops of phosphoric acid were added. Drug-loaded chitosan-heparin nanoparticles were obtained by adding 50 mL of the above chloroquine solution to 50 mL of chitosan-heparin solution. 2.5 mL of a 20% w/v sodium sulphate solution was added dropwise to the complete solution under magnetic stirring. This reaction was stirred during 1 hour at room temperature. Drug-conjugated chitosan nanoparticles were collected by centrifugation as described above.

3.6 Estimation of chloroquine loaded into chitosan-heparin nanoparticles

Chloroquine load on chitosan and chitosan-heparin nanoparticles was determined by spectrophotometry, measuring the absorbance of supernatants before and after disintegration of the nanoparticles by hydrochloric acid (HCl). 100 µL of nanoparticles were spun down at 17,530 rcf. Supernatant was discarded and the pellet was taken up in 100 µL of 0.1 M HCl and was kept at 4˚C overnight. The solution was centrifuged and the pellet resuspended again in 100 µL of 0.1 M HCl during 2 h at room temperature. After a new centrifugation, samples of all supernatants were analysed spectrophotometrically at a wavelength of 242 nm. Other samples were incubated for 10 days and the supernatant was analysed to measure the liberation of chloroquine after this period. All analyses were carried out in triplicate. Drug content was determined by comparing with a standard curve of chloroquine which was obtained from serial dilutions of chloroquine phosphate (between 0 and 0.75 mg/mL). As pH may have an effect in the absorbance, two calibration curves were calculated for the supernatants: one in water and another in hydrochloric acid. Nanoparticles were lyophilized in order to express the quantity of chloroquine per mg of NPs. Drug loaded NPs were characterized by DLS and SEM.

3.7 Plasmodium falciparum cell culture and growth inhibition assays

The *P. falciparum* 3D7 strain was grown *in vitro* in group B human RBCs. Briefly, parasites (thawed from glycerol stocks) were cultured at 37˚C in 75 cm^2 cell culture flasks (canted neck, Corning) containing RBCs in Roswell Park Memorial Institute (RPMI) complete medium, under a gas mixture of 92.5% N_2, 5.5% CO_2 and 2% O_2. Thin blood films were made every day from each culture flask, fixed with methanol, and stained for 10 minutes in Giemsa. For culture maintenance, parasitemias, calculated by counting the percentage of parasitized erythrocytes by light microscopy, were kept below 5% late

forms by dilution with washed RBCs. Growth factor was expressed as final parasitemia divided by initial parasitemia. For growth inhibition assays, parasitemia was adjusted to 1.5% with more than 90% of parasites at ring stage after sorbitol synchronization. This synchronization method, as described by Lambros and Vanderberg (22), is based on the differential permeability of the parasitized RBC membrane. While RBCs are naturally impermeable to sorbitol, infected RBCs with mature stages have a permeable membrane due to the structural modifications induced by the parasite. This property is used to selectively kill mature forms of the parasite by osmotic shock without affecting uninfected RBCs and RBCs parasitized by ring stages. 100 μL of infected *Plasmodium* culture were plated in 96-well plate and incubated in the presence of chitosan CQ-loaded NPs and chitosan-heparin CQ-loaded NPs for 48 h in the conditions described above. 500 μL of phosphate-buffered saline (PBS) and 4 μL of infected red blood cells with or without nanoparticles were mixed in a polystyrene test tube specifically designed for flow cytometry. Parasitemia was measured by flow cytometry after staining the DNA of pRBCs with 0.5 μL of a 0.5 mM solution of the nucleic acid dye Syto 11. For each sample, 50,000 cells were analysed with a BD FACSCalibur flow cytometer, equipped with a two-laser system, using the software CellQuestPro. Parasitemia was expressed as the percentage of infected red blood cells (% gated, proportion of cells marked with nuclear dye).

3.8 Statistical analysis

All data are expressed as means and standard deviations, indicated as "mean ± SD", of three independent replicates and the corresponding standard errors in histograms are represented by error bars. Differences were considered to be statistically significant when the p values were less than 0.05. Percentages of viability were obtained using non-treated cells as control of survival and IC_{50} values were calculated by nonlinear regression with

an inhibitory dose–response model using GraphPad Prism5 software (95% confidence interval). Concentrations were transformed using natural log for linear regression, and regression models were adjusted for the assayed replicates.

4. Ethical issues

Blood from voluntary donors was commercially obtained from the *Banc de Sang i Teixits* (www.bancsang.net) and blood was not collected specifically for this research; instead we used blood units that had been discarded for transfusion, usually because of an excess of blood relative to anticoagulant solution. Prior to their use, blood units undergo the analytical checks specified in the current legislation. Before being delivered to us, unit data are anonymized and irreversibly dissociated and any identification tag or label will have been removed in order to guarantee the anonymity of the blood donor. No blood data will be supplied, in accordance with the current *Ley Orgánica de Protección de Datos* and *Ley de Investigación Biomédica*. The PI (Dr. Fernàndez-Busquets) commits himself to not using the blood samples for studies other than those made explicit in this work, and to not forwarding them to other research groups. The proposal to which this master final project is associated was evaluated and approved by the Clinical Research Ethics Committee from the *Hospital Clínic de Barcelona*.

5. Results

5.1 Characterization, actual drug content and encapsulation efficiency

Chitosan has low solubility at neutral and alkaline pH. However, as it is a cationic polyelectrolyte polymer with ionizable amine groups, in an acidic environment the amine groups are positively charged. Therefore, chitosan tends to form intramolecular network structures by ionic cross-linking (electrostatic interactions) between NH_3^+ protonated groups and negatively charged counter ions of sodium sulphate, leading to the formation

of nanoparticles. The formation of nanoparticles is indicated by appearance of opalescence and increased density.

The synthesized chitosan-heparin particles were characterized by DLS and SEM analysis. Different chitosan-heparin ratios were tested in order to establish the most adequate regarding stability and size. DLS-determined particle size and polydispersity index indicated that the mean chitosan-heparin nanoparticle size was in the range of 290 - 450 nm. A chitosan/heparin ratio of 0.25:0.25 appeared to produce the smallest particle size (290 ± 7.45) (Table 1).

Loading of chloroquine into chitosan-heparin nanoparticles increased their size. The drug-loaded nanoparticle size was in the range of 400 - 700 nm (Table 2). Chloroquine was used at a concentration of 2 mg/mL based in pre-existing literature (16) (23). Chitosan was used at a concentration of 0.25 mg/mL as it seemed to produce the smallest size. Particle size is essential for efficient delivery since small structures are more likely to penetrate *Plasmodium*-infected erythrocytes. Heparin was tested at three different concentrations (0, 0.1 and 0.25 mg/mL). Nanoconjugate chloroquine was successfully prepared in a polymer:heparin:drug ratio of 0.25:0.25:2 (Table 2). Therefore, the nanoparticles prepared with this specific composition were used for the rest of the study.

Polydispersity in all different ratios of chitosan *vs.* heparin ranges from 0.07 to 0.01. It is very close to 0, which denotes a monodisperse system with low level of aggregation (Tables 1, 2).

Table 1. Mean hydrodynamic diameter (MHD) and polydispersity index (PDI) of chitosan/heparin nanoparticles at different concentrations.

Group	[Ch:Hep] (mg/mL)	MHD ± S.D. (nm)	PDI
1	0.5:0	584.2 ± 6.8	0.15 ± 0.03
2	0.25:0	185.5 ± 0.6	0.18 ± 0.01
1a	0.5:0.5	447.7 ± 3.0	0.14 ± 0.02
1b	0.5:0.25	393.1 ± 5.2	0.21 ± 0.03
2a	0.25:0.25	290.0 ± 7.5	0.20 ± 0.02
2b	0.25:0.1	447.8 ± 38.3	0.37 ± 0.07

Table 2. Mean hydrodynamic diameter (MHD) and polydispersity index (PDI) of CQ-loaded chitosan/heparin nanoparticles.

Group	[Ch:Hep:CQ] (mg/mL)	MHD ± S.D. (nm)	PDI
3	0.25:0:2	726.2 ± 7	0.09 ± 0.02
4	0.25:0.1:2	501.7 ± 11.4	0.28 ± 0.02
5	0.25:0.25:2	410.8 ± 2.2	0.2 ± 0.01

There are no significant differences between the drug content just after the synthesis and after an incubation period of 10 days of chitosan CQ-loaded NPs and chitosan-heparin CQ-loaded NPs (Table 3). Figure 1 in appendix A (supplementary data) shows the calibration curve of chloroquine in water (a) and in hydrochloric acid (b).

Table 3. Drug content of chitosan chloroquine-loaded and chitosan-heparin CQ-loaded nanoparticles.

	[CQ], mg/mg NPs After synthesis	[CQ], mg/mg NPs After 10 days
Ch-CQ NPs	11.88	11.86
Ch/hep-CQ NPs	12.28	12.25

Both chitosan nanoparticles and chitosan-heparin chloroquine-loaded nanoparticles were roughly spherical in morphology. SEM images of both types of nanoparticles are shown (Figure 2).
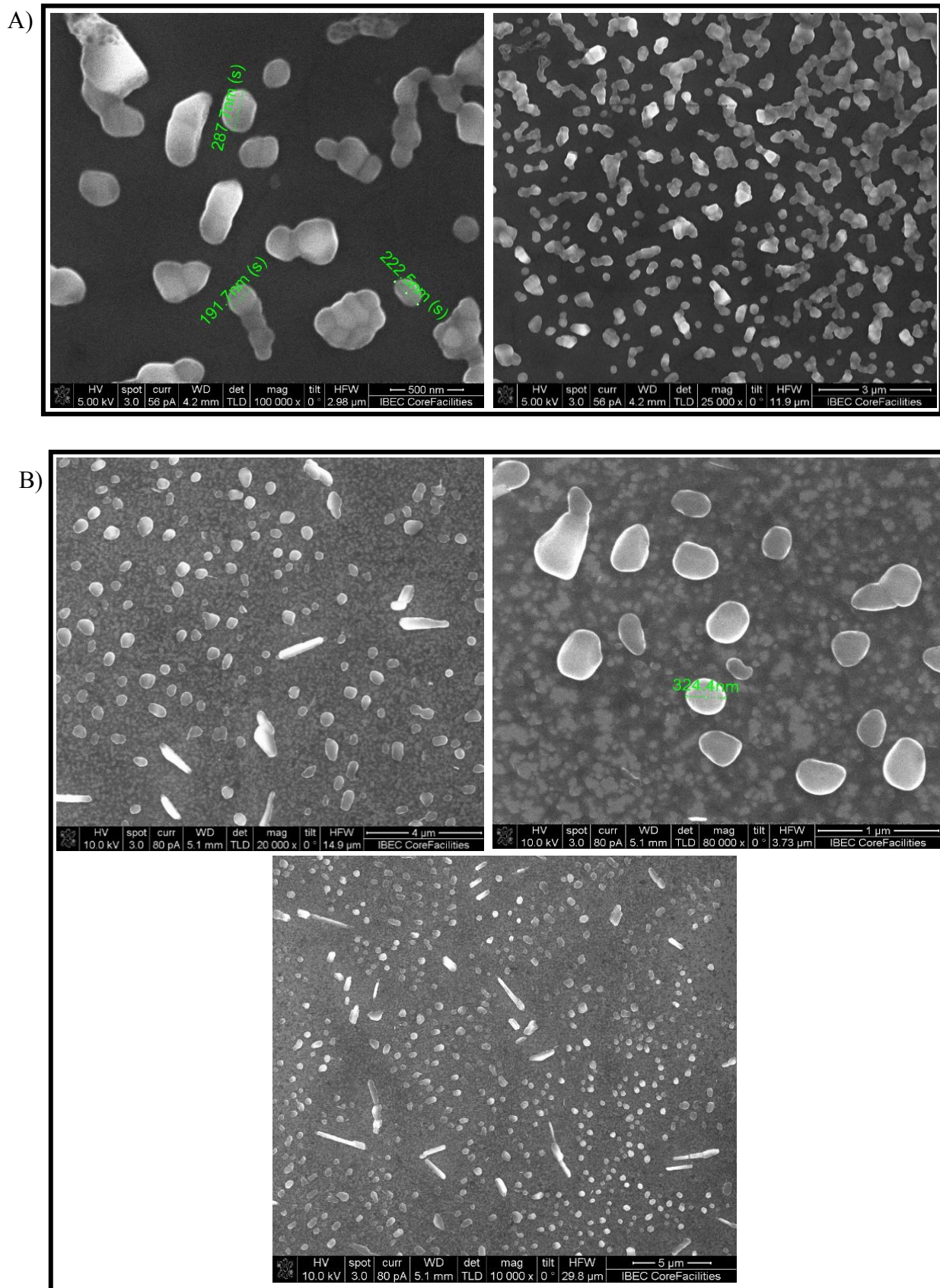
Fig. 2. SEM images of chitosan nanoparticles (A) and chitosan/heparin chloroquine-loaded nanoparticles (B)

5.2 Unspecific cytotoxicity of chitosan-heparin nanoparticles and drug-loaded nanoparticles

The cytotoxicity of chitosan-heparin and chitosan-heparin CQ-loaded nanoparticles on HUVEC cell lines was evaluated by assessing the cell viability using a standard MTT assay. Different concentrations of chitosan NPs, chitosan-heparin NPs, chitosan chloroquine-loaded NPs, chitosan-heparin chloroquine-loaded NPs and chloroquine were added to cells and incubated for 24 and 48 h. The percentage cell growth inhibition was reported as the percentage of surviving cells after specific periods of incubation. It was found that there were quite significant differences in cell viability among the cells treated with different nanoparticles and those treated with chloroquine (Fig. 3). Results for chloroquine follow a logical trend: the lower was the degree of toxicity with the lower drug concentration and lower cell viability after 48h than 24h. However, a dissimilar cell viability was observed for different nanoparticles at different times and concentrations. It seemed that nanoparticles with heparin show a higher cell viability than those without heparin. In consequence, these chitosan-heparin chloroquine-loaded nanoparticles are not expected to be safe for biomedical applications. Graphical representations of chitosan nanoparticles and chitosan-heparin nanoparticles *in vitro* cytotoxicity are shown in Figure 2 in appendix A (supplementary data).
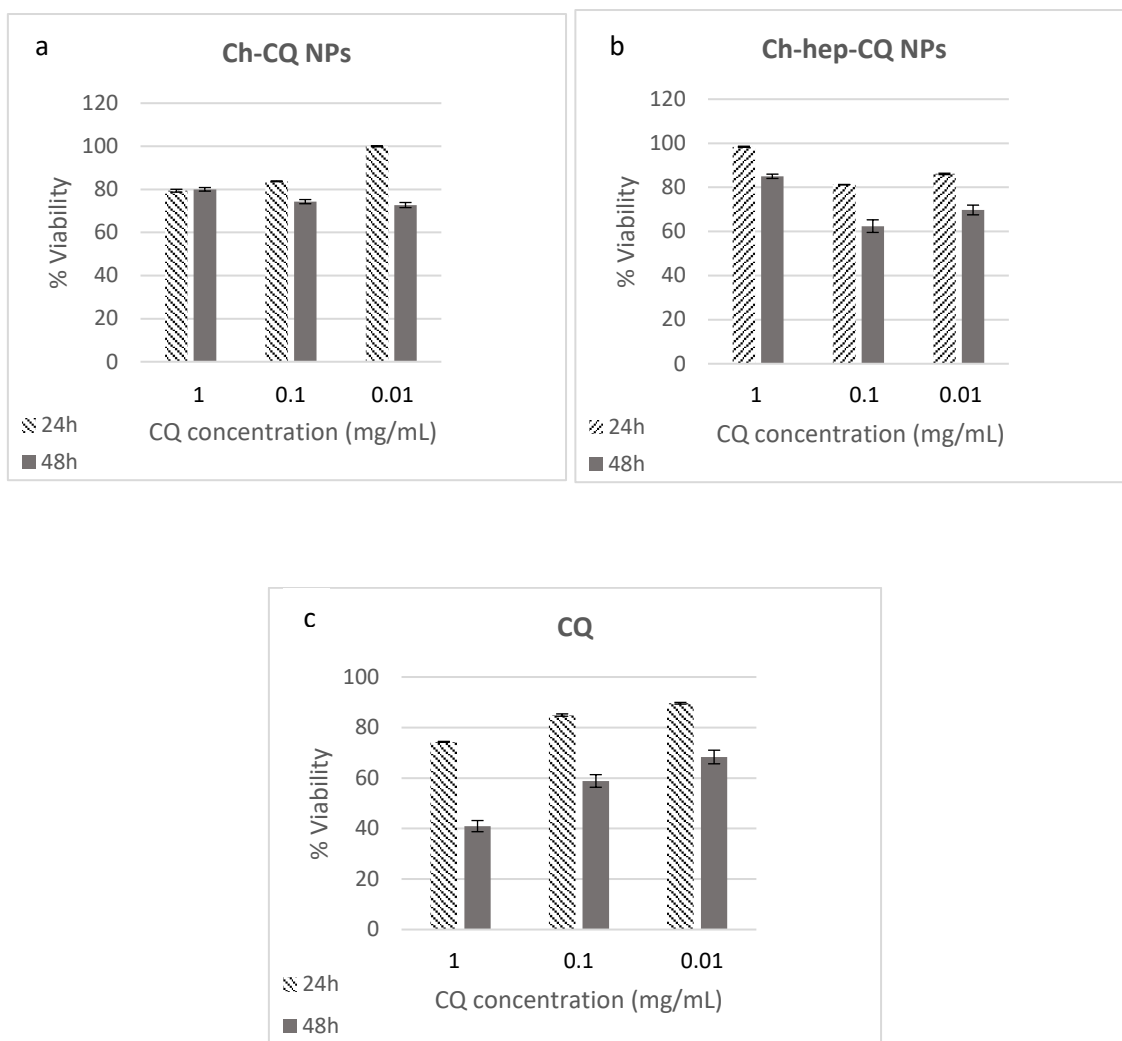
Fig 3. Graphical representation of *in vitro* cytotoxicity of chitosan CQ-loaded nanoparticles (a), chitosan-heparin CQ-loaded nanoparticles (b) and CQ (c) assessed by MTT assay.

5.3 Growth inhibition assays

The effectivity of chitosan CQ-loaded nanoparticles, chitosan/heparin CQ-loaded nanoparticles and CQ was assessed by growth inhibition assays. Parasites were cultured either in the absence -control group- or presence of different concentrations of CQ, either free or embedded in the nanoparticles. Concentrations of free CQ ranging from 10^4 ng/mL to 10^2 ng/mL resulted in approximately 100% inhibition of parasite growth. With CQ concentrations lower than 10 ng/mL, no inhibition of parasite growth was observed (Fig. 4). To calculate IC_{50} value of chloroquine, a dose-response curve was traced (Fig. 5). The IC_{50} for chloroquine against the 3D7 strain of *P. falciparum* ranges from 3.6

to 188.7 ng/mL (mean: 5.98 ng/mL). Referring to the efficacy of nanoparticles, it has been found that neither chitosan CQ-loaded nanoparticles nor chitosan-heparin CQ-loaded nanoparticles have antimalarial activity against *P. falciparum* (Fig. 4). Parasitemia in presence in both type of nanoparticles is similar to the one of the control (group without drug).
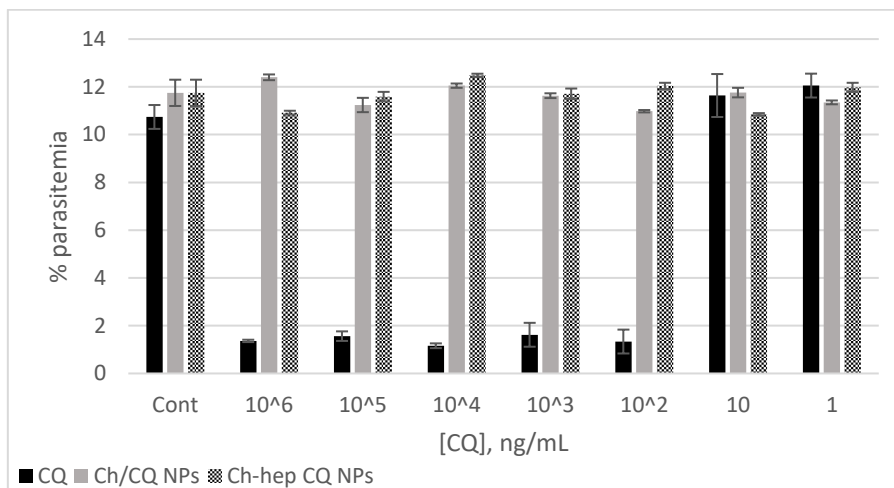

Fig. 4. Growth of *P. falciparum* 3D7 in erythrocytes incubated with different concentrations of CQ (black), Chitosan CQ-loaded nanoparticles (grey) and Chitosan-heparin CQ-loaded nanoparticles (dots) and in infected erythrocytes incubated in an identical way but in the absence of CQ and NPs (control).
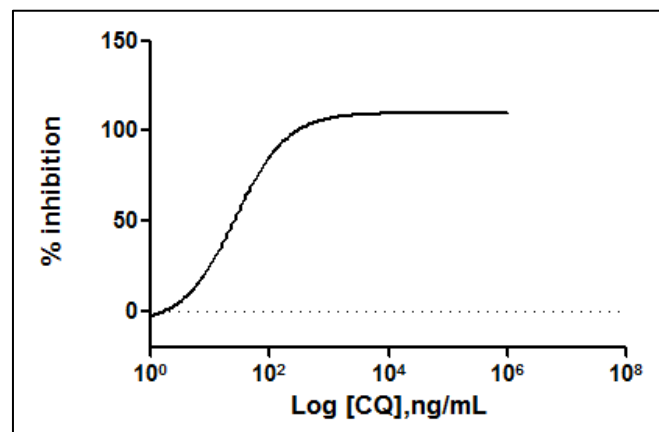

Fig. 5. Dose-response curve of different concentrations of chloroquine.

6. Discussion

Despite the lack of economic resources for research in malaria-oriented nanomedicines, many different nanocarriers have been developed. Nanocarriers have the potential to reduce the toxicity and to improve the bioavailability and biodistribution of certain drugs. The success of any drug delivery system depends upon the physicochemical interaction with the biological system to deliver its drug cargo at the optimum rate and at the site where it is needed. In this study, chitosan-heparin nanoparticles and conjugated CQ are examined as a potential antimalaria therapy.
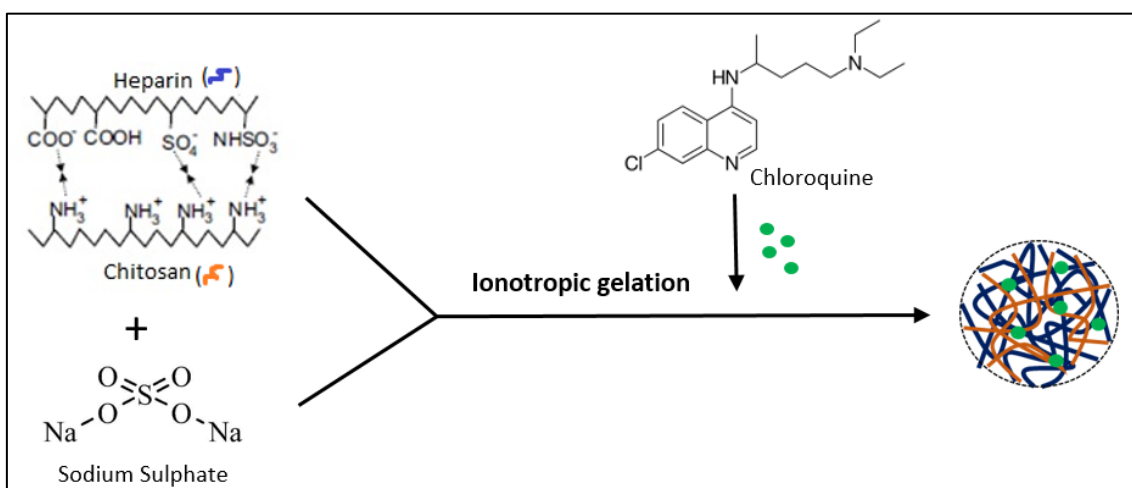

Figure 6. Schematic representation of the chemical structure of chitosan, of its interaction with sodium sulphate and heparin and of its conjugation with chloroquine.

Chitosan-heparin nanoparticles were synthetized by the ionotropic gelation method (Fig 6). The average hydrodynamic diameters of chitosan-heparin nanoparticles and CQ-loaded chitosan-heparin nanoparticles have a relatively narrow size distribution, within the range of 290 – 447 nm and 410 – 725 nm, respectively. These results suggest an increment in particle size after the incorporation of both heparin and chloroquine. Furthermore, nanoparticles seem to be larger in size as indicated by DLS measurements in comparison to particle size determination from SEM images (Fig. 2). To carry out SEM analysis, nanoparticles were measured in dry state whereas DLS measurements were

expected to give the average hydrodynamic radius rather than the actual size of the nanoparticles. Both CQ-loaded chitosan nanoparticles and CQ-loaded chitosan/heparin nanoparticles are stable at room temperature. Although some SEM images show certain aggregation of the nanoparticles (Fig. 2) -they are easily distinguished-, usually nanoparticles do not aggregate upon storage.

After a first introductory experiment using fluorescence confocal microscopy, no specific targeting to late forms of infected erythrocytes was found (results not shown). Heparin might be tightly embedded in the chitosan matrix and therefore, reactive groups are not exposed on the surface of the nanoparticles. In order to overcome this problem, heparin can be used to coat the surface of the nanoparticles. Previous studies reported that heparin formed a loose network around nanoparticles, rather than a tightly bound layer. This electrostatically bound heparin is prone to peel off from nanoparticle surfaces, incurring the risk of anticoagulation and internal bleeding while in the blood circulation (21). Hence, subsequent strategies must focus on heparin covalently bound to the surface of the nanoparticles. Apart from this formulation, new approaches varying the quantity or encapsulation of heparin or even sodium sulphate (counter ion) must be investigated in order to overcome the problem of non-specific cytotoxicity of the nanoparticles. As it was previously shown, nanoparticles present certain degree of cytotoxicity, which seemed to be lower in those nanoparticles containing heparin. Cytotoxicity might be the due to the presence of chitosan free amine groups. Heparin blocks some positive surface charges of chitosan and for this reason cytotoxicity appeared to be lower in presence of heparin. However, heparin molecule attachment did not sufficiently suppress all free amine groups and some of the them are still free, conferring, therefore, certain degree of non-specific cytotoxicity to the nanoparticles.

After formulation and characterization of chitosan-heparin nanoparticles, CQ was loaded into them. However, no inhibition of parasite growth was induced by these CQ-containing nanoparticles. The amount of CQ in the supernatants just after the synthesis and after an incubation period of 10 days was the same, indicating that, under the used experimental conditions, CQ is not released from the nanoparticles and therefore, cannot exert its effect as antimalarial. In consequence, intravenous delivery formulations are not recommended for this structures and new alternative approaches must be developed. (i) Encapsulating drugs chemically different from CQ could offer better release patterns. (ii) Chitosan drug-loaded nanoparticles could be adequate for oral administration: the synthesised nanoparticles are degraded under laboratory conditions in 0.1 M HCl; as human gastric fluid contains HCl, nanoparticles may be degraded in the stomach releasing encapsulated CQ. Nevertheless, chitosan has been widely used for oral drug delivery systems because of its excellent mucoadhesive and absorption-enhancing properties (24). As Akhtar F. *et al.* reported, chitosan nanoparticles positively influence curcumin transport across mucosal surfaces and protect this drug from degradation, enhancing its bioavailability and half-life in plasma (25). Therefore, a similar effect could be expected for chloroquine and other drugs, ensuring a sustained release of the drug over more hours post feeding. (iii) Another largely unexplored approach is the delivery of chitosan drug-loaded nanoparticles to vector mosquitoes to target the parasite stages in the insect vector itself. Strategies that control malaria using direct action against the mosquito are not new, but most of them aim at eliminating the vector. One of the most important stages of *Plasmodium* development in the mosquito is the ookinete, which appears in the mosquito midgut between 16 and 20 h after bloodmeal ingestion and its outcome determines the success of malaria transmission. The first barrier that the ookinetes face during their migration through the midgut wall is the chitinaceous peritrophic matrix, an extracellular

layer that coats the apical side of the midgut epithelium. To cross this barrier, it has been shown that ookinetes secrete chitinase, an enzyme that hydrolyses chitin and chitosan (26) (27) (28). Afterwards, as an essential step of host midgut epithelial cell invasion, some *Plasmodium* ookinetes bind proteoglycans such as chondroitin sulphate. Although there is no evidence for the existence of glycosaminoglycans (GAGs) such as heparin in the mosquito midgut, it has also been demonstrated that some ookinete proteins do bind to heparin *in vitro* (21) (29). Therefore, heparin may be adequate to target antimalarial-loaded nanovectors to *Plasmodium* mosquito stages. Given the endogenous nature of chitosan in the mosquitoes and the expected lack of susceptibility of these insects to the presence of blood anticlotting agents, nanoparticles are likely to be innocuous for *Anopheles*. In this context, chitosan/heparin nanoparticles would be loaded with the drug atovaquone, as it has been reported to have antimalarial activity against ookinetes (30) (31). Basically, targeted nanocarriers are formed by three elements: nanocapsule, targeting molecule and the drug itself (chitosan, heparin and chloroquine, respectively, in this study). As mentioned above, in order to obtain different frameworks better suited to each specific situation, those elements can be exchanged. Consequently, more studies are required to further optimize the rate of release of current and future compounds.

New approaches are required to further optimize the scarce resources available for malaria control and elimination. The implementation of novel delivery approaches is less expensive than the process leading to the discovery of new drugs. Additionally, using an economically affordable molecule such as heparin, which presents synergistic activity as antimalarial and as a targeting molecule of nanocarriers to pRBC and thus lowering the IC_{50} of drugs, will contribute to reaching a cost-effective design for nanocarriers (15). Finally, delivering antimalarial drugs exclusively to the mosquito vectors may also reinforce the idea of reducing costs because the clinical trials otherwise required for

treatments administered to people could be simplified. Although the results presented here are not as good as we expected, they are a promising starting point in the context of the current malaria socioeconomic and pharmacotherapy scenario outlined above.

7. Conclusions

In this study, chitosan/heparin nanoparticles loaded with chloroquine were prepared based on an optimized ionotropic gelation method, which employed sodium sulphate as a cross-linker. The optimum concentrations obtained were 0.25 mg/mL chitosan, 2.5 mg/ mL heparin, 20% w/v sodium sulphate, 1% w/v kolliphor and 2 mg/mL chloroquine. Under those conditions, chitosan-heparin nanoparticles were obtained with acceptable PDI and size range of 290 – 450 nm. Drug loaded nanoparticles appeared to be bigger (within the range of 400 – 700 nm). Nanoparticles present certain degree of cytotoxic activity based on MTT assays, probably due to chitosan free amine groups. No *in vitro* release of chloroquine was observed and therefore there is no inhibition of parasite growth. Hence, further studies are required to overcome those problems and to ensure the release and activity of the encapsulated antimalarial drug.

References

1. WHO | Malaria. WHO. 2016;

2. CDC - Malaria. 2016.
   Available from: https://www.cdc.gov/malaria/

3. WHO | Fact Sheet: World Malaria Report 2016. WHO.

4. Cibulskis RE, Alonso P, Aponte J, Aregawi M, Barrette A, Bergeron L, et al. Malaria: Global progress 2000 - 2015 and future challenges. Infect Dis poverty 2016;5(1):61.
   Available from: http://www.ncbi.nlm.nih.gov/pubmed/27282148

5. Draper SJ, Angov E, Horii T, Miller LH, Srinivasan P, Theisen M, et al. Recent advances in recombinant protein-based malaria vaccines. Vaccine 2015;33(52):7433–43.
   Available from: http://dx.doi.org/10.1016/j.vaccine.2015.09.093

6. WHO | Antimalarial drug resistance. WHO. 2014;

7. Sinha S, Medhi B, Sehgal R. Challenges of drug-resistant malaria. Parasite. 2014;21:61.
   Available from: http://www.parasite-journal.org/10.1051/parasite/2014059

8. European Commission. Research&Innovation. Nano in Healthcare - Nanotechnology applications - Research & Innovation - Key Enabling Technologies - European Commission.
   Available from: http://ec.europa.eu/research/industrial_technologies/nano-in-healthcare_en.html

9. Nature Nanotechnology - nanotechnology facts and figures.
   Available from: http://www.nature.com/nnano/nanofacts/index.html

10. Mg K, Krenn V, Huebner F, Wagner W, Resch R. History and Possible Uses of Nanomedicine Based on Nanoparticles and Nanotechnological Progress. J Nanomed Nanotechnol. 2015;64172(6):3362157–7439.
    Available from: http://dx.doi.org/10.4172/2157-7439.1000336

11. Kreuter J. Nanoparticles-a historical perspective. Int J Pharm. 2007;331(1):1–10.

12. Santos-Magalhães NS, Mosqueira VCF. Nanotechnology applied to the treatment of malaria. Adv Drug Deliv Rev. 2010;62(4–5):560–75.
    Available from: http://dx.doi.org/10.1016/j.addr.2009.11.024

13. Pirson P, Steiger RF, Trouet A, Gillet J, Herman F. Liposomes in the chemotherapy of experimental murine malaria. Trans R Soc Trop Med Hyg. 1979;73(3):347.
    Available from: http://www.ncbi.nlm.nih.gov/pubmed/382476

14. Singhal A, Gupta CM. Antibody-mediated targeting of liposomes to red cells in vivo. FEBS Lett. 1986;201(2):321–6.

15. Marques J, Moles E, Urbán P, Prohens R, Busquets MA, Sevrin C, et al. Application of heparin as a dual agent with antimalarial and liposome targeting activities toward Plasmodium-infected red blood cells. Nanomedicine Nanotechnology, Biol Med. 2014;10(8):1719–28.
Available from: http://dx.doi.org/10.1016/j.nano.2014.06.002

16. Tripathy S, Das S, Chakraborty SP, Sahu SK, Pramanik P, Roy S. Synthesis, characterization of chitosan–tripolyphosphate conjugated chloroquine nanoparticle and its in vivo anti-malarial efficacy against rodent parasite: A dose and duration dependent approach. Int J Pharm. 2012;434(1–2):292–305.
Available from: http://linkinghub.elsevier.com/retrieve/pii/S0378517312005844

17. N MD, Eskandari R, Zolfagharian H, Mohammad M. Preparation and in vitro characterization of chitosan nanoparticles containing Mesobuthus eupeus scorpion venom as an antigen delivery system. J Venom Anim Toxins Incl Trop Dis. 2012;18(1):44–52.

18. Rampino A, Borgogna M, Blasi P, Bellich B, Cesàro A. Chitosan nanoparticles: Preparation, size evolution and stability. Int J Pharm. 2013;455(1–2):219–28.
Available from: http://dx.doi.org/10.1016/j.ijpharm.2013.07.034

19. Kobayashi K, Takano R, Takemae H, Sugi T, Ishiwa A, Gong H, et al. Analyses of Interactions Between Heparin and the Apical Surface Proteins of Plasmodium falciparum. Sci Rep. 2013;3:573–80.
Available from: http://www.nature.com/articles/srep03178

20. Valle-Delgado JJ, Urbán P, Fernàndez-Busquets X. Demonstration of specific binding of heparin to Plasmodium falciparum-infected vs. non-infected red blood cells by single-molecule force spectroscopy. Nanoscale. 2013;5(9):3673–80.
Available from: http://www.ncbi.nlm.nih.gov/pubmed/23306548

21. Marques J, Valle-Delgado JJ, Urbán P, Baró E, Prohens R, Mayor A, et al. Adaptation of targeted nanocarriers to changing requirements in antimalarial drug delivery. Nanomedicine. 2016.
Available from: http://www.ncbi.nlm.nih.gov/pubmed/27720930

22. Lambros C, Vanderberg JP. Synchronization of Plasmodium falciparum erythrocytic stages in culture. J Parasitol. 1979;65(3):418–20.
Available from: http://www.ncbi.nlm.nih.gov/pubmed/383936

23. Tripathy S, Chattopadhyay S, Dash SK, Ray Chowdhuri A, Das S, Sahu SK, et al. Chitosan conjugated chloroquine: Proficient to protect the induction of liver apoptosis during malaria. Int J Biol Macromol. 2015;74:585–600.
Available from: http://dx.doi.org/10.1016/j.ijbiomac.2014.12.016

24. Sogias IA, Williams AC, Khutoryanskiy V V. Why is Chitosan Mucoadhesive? Biomacromolecules. 2008;9(7):1837–42.
Available from: http://pubs.acs.org/doi/abs/10.1021/bm800276d

25. Akhtar F, Rizvi MMA, Kar SK. Oral delivery of curcumin bound to chitosan nanoparticles cured Plasmodium yoelii infected mice. Biotechnol Adv. 2012;30(1):310–20.
Available from: http://dx.doi.org/10.1016/j.biotechadv.2011.05.009

26.   Langer RC, Vinetz JM. Plasmodium ookinete-secreted chitinase and parasite penetration of the mosquito peritrophic matrix. Trends Parasitol. 2001;17(6):269–72.

27.   Shahabuddin M. Plasmodium ookinete development in the mosquito midgut: a case of reciprocal manipulation. Parasitology. 1998;116(1998):S83-93.
        Available from: http://www.ncbi.nlm.nih.gov/pubmed/9695113

28.   Vlachou D, Schlegelmilch T, Runn E, Mendes A, Kafatos FC. The developmental migration of Plasmodium in mosquitoes. Curr Opin Genet Dev. 2006;16(4):384–91.

29.   Dinglasan RR, Alaganan A, Ghosh AK, Saito A, van Kuppevelt TH, Jacobs-Lorena M. Plasmodium falciparum ookinetes require mosquito midgut chondroitin sulfate proteoglycans for cell invasion. Proc Natl Acad Sci USA. 2007;104(40):15882–7.

30.   Butcher GA, Mendoza J, Sinden RE. Inhibition of the mosquito transmission of Plasmodium berghei by Malarone (atovaquone-proguanil). Ann Trop Med Parasitol. 2000;94(5):429–36.
        Available from: http://www.ncbi.nlm.nih.gov/pubmed/10983555

31.   Fowler RE, Sinden RE, Pudney M. Inhibitory activity of the anti-malarial atovaquone (566C80) against ookinetes, oocysts, and sporozoites of Plasmodium berghei. J Parasitol. 1995;81(3):452–8.
        Available from: http://www.ncbi.nlm.nih.gov/pubmed/7776134

Benefits of research, applicability and validity

As result of this study, an optimized protocol for the synthesis of drug-loaded nanoparticles with acceptable PDI and size range was established. Based on this protocol, different types of nanoparticles for targeted drug delivery can be obtained by exchanging the three former components of the nanocarriers: nanocapsule, targeting molecule and drug. Therefore, synthesised nanoparticles can be adapted to different situations, being more appropriate for each specific use. Additionally, referring to economic aspects, implementation of new delivery methods is usually cheaper than finding new antimalarial drugs. Drug-loaded nanoparticles have several applications that range from oral delivery to direct delivery of drugs to mosquitoes. For oral delivery purposes, chitosan nanoparticles enhance the bioavailability and half-life in plasma of the drug loaded as well as ensuring a sustained release of it. The strategy of direct administration to

mosquitoes will bypass or at least reduce clinical trials as it is not designed for human administration.

However, more studies are required. It is necessary to corroborate previous data about heparin targeting to pRBCs. Before the complete implementation of chitosan/heparin drug-loaded nanoparticles, further steps must be done. For example, *in vivo* assays.

Work plan

| Activity	Timeline								
Activity	October	November	December	January	February	March	April	May	June
Literature reviewing	X	X	X	X	X	X	X	X	X
Protocol optimization		X	X	X	X	X			
Learning techniques	X	X	X	X	X	X	X		
NPs' sythesis			X		X		X	X	
NPs characterization			X	X		X	X		
CQ loading					X	X			
GIAs								X	X
MTT assay							X	X	X
Proposal			X	X					
Project Writing							X	X	X

Acknowledgments

I would like to thank all the people who contributed in some way to the work of this Master Final Project. First, I would like to gratefully and sincerely thank my supervisor Dr. Xavier Fernández Busquets for his guidance and understanding. Thank you for his confidence and for giving me the opportunity to be part of the great Nanomalaria research group. I would also like to thank all the members of this group. Especially Arnau, Elena, Laura and Miriam for their support, patient and time. Thank you for all the help and for their enriching observations and advices. I have gained a lot with their knowledge and experience. I would also like to thank all of them for their enthusiasm and entertainment, even during difficult moments, contributing to create a nice laboratory environment.

Thanks to all the teachers, colleagues and friends from the Master. Sharing laughs and stressful moments with them, made this year and master much more bearable.

And last but not least, thanks to my friends and family. Thank you to my friends in Barcelona and the others in Salamanca and around the world for all your support. Thank you for helping me to disconnect in stressful moments and thank you for being there, even in the distance. *Gracias a mi familia, especialmente a mis padres y a mi hermana Elena, por su desinteresado apoyo y ánimos. Mil gracias por haberme dado la oportunidad de estudiar e impulsar mis primeros pasos en el mundo de la investigación, ya que literalmente y sin que suene a tópico, sin ellos no hubiera sido posible.*

Appendix A

Supplementary data

Figure 1. Calibration curve of chloroquine phosphate in water (A) and in hydrochloric acid (B)

A — Calibration curve (H$_2$O)
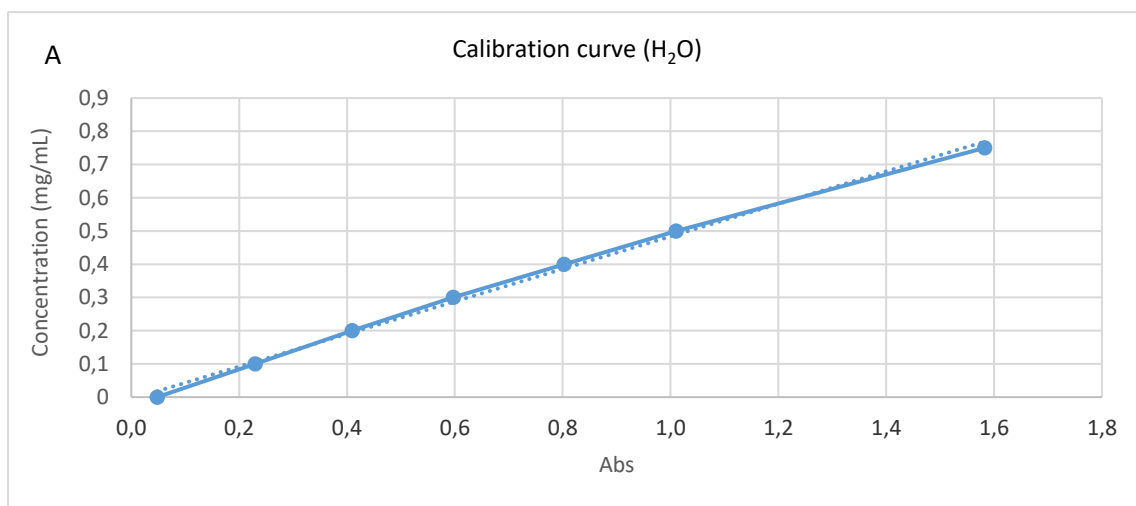
Equation: y = 0.4895 x – 0.0059
R = 0.9969

B — Calibration curve (0.1 M HCl)
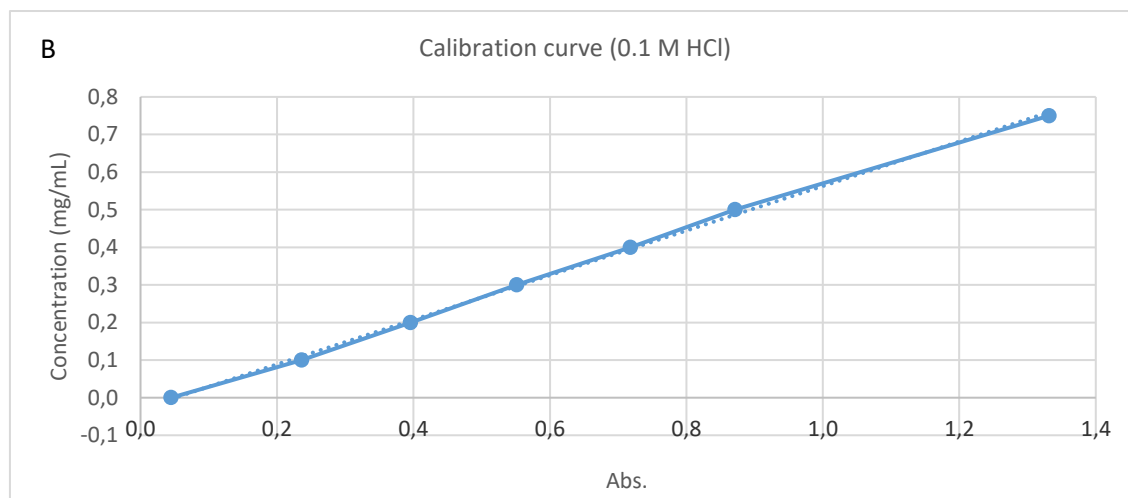
Equation: y = 0.5927 x – 0.0299
R = 0.9989

Figure 2. Graphical representation of *in vitro* cytotoxicity of chitosan NPs (a) and chitosan-heparin NPs (b) by MTT assay.